Journal of Applied Polymer Science

A novel conductive membrane with RGO/PVDF coated on carbon fiber cloth for fouling reduction with electric field in separating polyacrylamide

Yuehua Zhang,[1] Lifen Liu,[1,2] Fenglin Yang[1]

[1]Key Laboratory of Industrial Ecology and Environmental Engineering (MOE), School of Environmental Science and Technology, Dalian University of Technology, Dalian 116024, China

[2]School of Food and Environment, Dalian University of Technology, Panjin 124221, China

Correspondence to: L. Liu (E-mail: lifenliu@dlut.edu.cn)

ABSTRACT: Directly applying an electric field on conductive membrane can effectively mitigate membrane fouling. Thus, a conductive reduced graphene oxide/polyvinylidene fluoride (RGO/PVDF) membrane was prepared by casting PVDF and graphene oxide (GO) solution over a selected carbon fiber cloth, then phase inversion and final heat treatment in hydroiodic acid (HI) solution. This method realized uniform and stable presence of RGO in PVDF membrane. Scanning electron microscopy (SEM) images showed addition of GO reduced the pore size of the composite membranes. The thermal HI treatment partially reduced graphene oxide to RGO, and made the membrane more conductive but less hydrophilic [as characterized by Fourier transform infrared spectroscopy (FTIR), Raman spectroscopy, and contact angle (CA)]. From thermogravimetric analysis (TGA), it showed that the addition of GO and RGO improved the thermal stability of the membranes, when temperature was lower than 400 °C. The HI treatment increased the pore size and water flux of the RGO/PVDF membrane (being 71.6% higher than the GO/PVDF membrane). The RGO/PVDF membrane was used in separating polyacrylamide (PAM), a macromolecule pollutant in oil field waste water; when applying a 0.6 V/cm external electric field, its membrane fouling and flux decline was effectively slowed down, as shown in the fitting curves slopes using the classical cake filtration model (t/V–V). Being uniform and stable, the RGO/PVDF membrane had great potential for practical applications.
 J. Appl. Polym. Sci. **2016**, *133*, 43597.

KEYWORDS: applications; conducting polymers; membranes; separation techniques

Received 26 November 2015; accepted 4 March 2016
DOI: 10.1002/app.43597

INTRODUCTION

Membrane separation is widely used in many industries[1–5] because it is more efficient than conventional separation methods. However, the inevitable membrane fouling is a barrier for cost-effective operation. To combat the adverse effect of fouling, frequent physical/chemical cleaning is required, which not only increased the costs but also complicated the operation. Thus, intensive and extensive methods studies about membrane fouling reduction had been conducted,[6–8] including the use of electric field.[9–21] The energy cost of using high-intensity electric field in ultrafiltration is higher[9,10] than using low-intensity minute electric field.

To improve fouling reduction efficiency, applying directly a low-intensity electric field to conductive membranes has been studied and proved effective. But, there are no low-cost and commercially available conductive membranes in water treatment sector, besides the expensive carbon membrane and metal membrane. Low-cost conductive membranes, their preparations and uses as electrode membranes, the possible integrations of electrocatalysis or electricity-induced fouling reduction have not been extensively explored.

Electricity conductive composite membranes could be prepared by loading carbon nanotube on membrane surface[11,12] or blending in polymer casting solution.[13,14] The blended polysulfone membrane had nitrogen doped or phosphorus-doped carbon nanotube which negatively charged the surfaces of composite membrane, increased salt rejection, and antifouling resistance.[15] Conductive bases such as carbon fiber cloth or stainless-steel mesh had been used in preparing conductive membrane, by coating PVDF and conductive polymers onto it[16,17] to improve the filtration property. Nonconductive nonwoven filter/cloth had also been used and modified with conductive polymers (polyaniline, polypyrrole),[18,19] and graphene doping further improved the conductivity.[20,21]

Studies had reported the use of electric conductive membrane under minute electric field, provided by iron anode or bioanode, reduced membrane fouling. Especially, when the membrane was used as cathode in coupled membrane bioreactor (MBR)–microbial fuel cell (MFC) reactors, the sustained electric field reduced fouling of cathode membranes (modified stainless-steel mesh and/or carbon fiber cloth),[22,23] and produced certain electrical energy.

In this study, the preparation of low-cost novel conductive membrane using low-cost carbon fiber cloth, graphene, and PVDF became our target. Graphene oxide can dissolve in some solvents and disperse uniformly, when doped in solids, it has new application, for example, as fire retardants for epoxy resin.[24] As to reduced graphene oxide, it has great conductivity, which helps to improve the conductivity of composites,[20,21,25,26] so it is a good choice for preparing conductive membrane. Compared with polyethersulfone, polyamide, and other polymer materials, PVDF has better mechanical strength, corrosion, and heat resistance. The coating of PVDF and graphene oxide can narrow the pore size and improve conductivity. For stable operation, it is necessary to prepare membranes with the right pore size, better rejection, and uniform conductivity, and prevent possible shedding and aggregation of conductive component, which might negatively affect membrane performance.

For uniform dispersion of conductive substance in membrane, graphene oxide is dispersed in PVDF casting solution, and phase inversion is used for loading conductive components onto carbon fiber cloth. The prepared GO/PVDF membrane was treated with HI solution to reduce GO to RGO for more conductive RGO/PVDF membrane. The rejection performance and antifouling property of the RGO/PVDF membranes in separation of polyacrylamide (PAM) were studied under an externally supplied electric field.

PAM is selected as a model macromolecule pollutant because it is widely used in oil mining for enhancing oil recovery, a major pollutant in waste water from oil field. Since it negatively affects wastewater treatment with membranes for being viscous, it is difficult to separate and recover, its presence and its degradation product impacts water quality and poses environmental health problem.[27]

MATERIALS AND METHODS

Materials

Carbon fiber cloth was purchased from Ruibang Fiber Products co., Ltd. (240 g m^{-2}, Yixing, China), PVDF (FR904, Mr $\approx$ 600,000) was from Aifu Materials Co., Ltd. (Shanghai, China), graphite powder (CR) was from Sinopharm Chemical Regant Co., Ltd. (Tianjin, China). The chemicals used include polyvinylpyrrolidone (PVP-K30, Mr = 10,000–70,000), *N*,*N*-Dimethylformamide (DMF), sodium nitrate ($NaNO_3$), phosphorus pentoxide (P_2O_5), potassium persulfate ($K_2S_2O_8$), concentrated sulfuric acid (H_2SO_4, 98 wt %), potassium permanganate ($KMnO_4$), hydrochloric acid (HCL, 36 wt %), hydrogen peroxide (H_2O_2, 30 wt %), hydriodic acid (HI, 45 wt %) were purchased from Dalian Chemical Reagent Factory. They were all of analytical grade (AR).

Membrane Preparation

Graphene oxide (GO) was prepared from graphite powder using Hummer's method as reported.[28] GO/PVDF membrane was fabricated via casting and phase inversion. First, the casting solution was prepared by weighing 35.3 g of DMF and 0.5 g GO in Erlen-Meyer flask, keep it sealed, ultrasonic treatment was applied to dissolve GO in DMF. Second, 5 g PVDF and 0.84 g PVP (as pore-forming agent) were added to the above solution, stirred for 12 h. After degassing in a vacuum oven, the solution was casted on a piece of carbon fiber cloth, which was fixed on glass plate, using a gap distance of 150 μm (KTQ-Π. Shanghai Pushen Chemical Machinery Co. Ltd.) to form a thin coating layer. After 30 s exposure in air, the carbon cloth with coating and the glass plate were immersed in a deionized (DI) water bath overnight, and thus, the preparation of GO/PVDF membrane was completed. The control PVDF membrane was prepared similarly as described above without GO addition in DMF.

Further, GO was partially reduced by treatment in HI solution.[29–31] The wet membrane was cut into proper size, its surface was wiped with dry filter paper to remove excess water. Certain volume HI solution (enough for the membrane immersion) was put in a beaker and heated in 100 °C water bath. GO/PVDF membrane was immersed into the hot and excess HI solution for about 60 s, and then took out using tweezers. Afterward, it was repeatedly washed with alcohol, before final immersion in deionized water. The HI-reduced membrane was labeled as RGO/PVDF membrane.

Membrane Characterization

The surface morphologies of GO/PVDF and RGO/PVDF membrane were visualized by scanning electron microcosmic (SEM, NOVA NanoSEM 450, USA). FTIR spectrometer (EQUINOX 55, Germany) was used to investigate the changes of functional groups after HI reduction. The water contact angles of the prepared membranes were measured with a video-supported contact angle measurement instrument (OCA 20, Data physics, Germany). Raman spectroscopy (Raman, Axiovert 25, United Kingdom) used a YAG laser with an 532 nm excitation wavelength as the excitation source. Thermogravimetric analysis (TGA, SII TG/DTA 6300, Japan) was carried out on the composite membranes to estimate the membrane thermal stability. All the samples tested were dried in a vacuum oven (DZF-6000, Shanghai, China) at 40 °C for 48 h.

The electrical resistance of the prepared membranes was measured by digital multimeter (Victor VC 830 L). Fixing one probe on the carbon fiber cloth, and another one on the surface of the membrane after storage in deionized water. We report an average value of five pairs of measurements.

Membrane Filtration Properties and Flux Recovery Rate

Filtration flux of the membranes was determined under a constant transmembrane pressure (TMP) at 9.8 kPa. Using deionized water or PAM sample solution, the flux was measured in regular intervals of 5 min. The flux was calculated as follows:

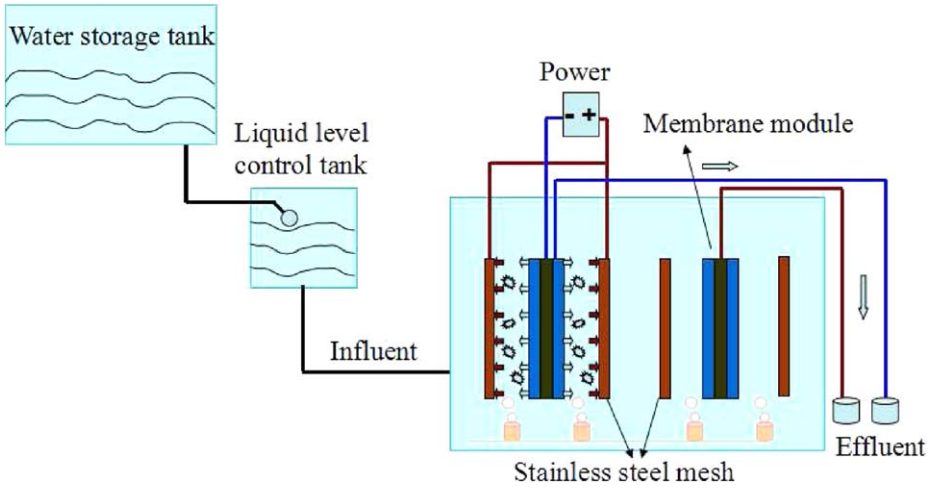

Figure 1. Configuration of the filtration system. [Color figure can be viewed in the online issue, which is available at wileyonlinelibrary.com.]

$$F = \frac{V}{\Delta t \cdot A}$$

Where F is the filtration flux (L m^{-2} h^{-1}), V is the accumulated water volume in 5 min (L), Δt is the filtration time (h), and A is the effective area of the membrane filtration (m^2).

Flux recovery rate (FRR) is the ratio of the flux of deionized water for the fresh membrane and the membrane after cleaning, and it is used to evaluate the performance of membrane fouling resistance. The formula is

$$FRR = \frac{F_{W2}}{F_{W1}}$$

Where F_{w1} is the deionized water flux of membrane which is fresh (L m^{-2} h^{-1}), and F_{w2} is the deionized water flux of membrane after filtration and physical cleaning (L m^{-2} h^{-1}). High FRR value indicated a higher antifouling properties of the membrane.[32]

Evaluation of the Membrane Performance with or without Electric Field

Polyacrylamide (PAM, Tianjin Damao Chemical Reagent Factory) was used as model foulant to evaluate antifouling performance of different membranes. PAM solution (0.4 g/L) was prepared and stirred to ensure complete dissolution. Appropriate sized GO/PVDF and RGO/PVDF membrane module (the effective filtration area of membrane was 6 × 5 cm) was installed in reactor, with stainless-steel mesh as the anode. By measuring the flux changes and rejection, the performance of membrane under an applied electric field (0.6 V/cm) or not (0 V/cm) was compared (Figure 1). Each membrane filtration test was repeated three times. After each cycle, the fouled membranes were cleaned by simple water flushing.

RESULTS AND DISCUSSION

Properties of Prepared Membrane

The surface morphology of the prepared membrane was observed (scanning electron microscope (SEM) images, Figure 2). Comparing (b) with (c), the RGO/PVDF membrane was more porous than GO/PVDF membrane. The cross-section image of RGO/PVDF membrane had more irregular pores (d–f). There was no obvious finger-shaped ones, but slightly stretched pore due to the added GO. GO in casting solution (0.1 wt %) increased solution viscosity, entailed a slower phase inversion, which led to smaller pores.[33] The only difference between GO/PVDF and RGO/PVDF membrane was caused by the thermal treatment in HI solution, so the observed larger pore size of RGO/PVDF membrane was due to the treatment of HI solution and structural changes of GO/PVDF membrane.

As shown in Figure 3, for the GO/PVDF membrane, the contact angle was 76.5 ± 1.7°, lower than the RGO/PVDF membrane. This is caused by the added graphene oxide (GO) and the presence of abundant oxygen-containing functional groups, such as hydroxyl, carboxyl, epoxy groups, and so on. It had higher hydrophilicity.[34] After reduction with hydriodic acid solution, some oxygen-containing functional groups were destroyed, and this resulted in the weaker hydrophilicity (b). It was found that reduced graphene oxide could modify cottons as hydrophobic material to remove oils from water.[35] This result was consistent with the weak hydrophilicity. However, the water flux was higher for RGO/PVDF, for the larger pore size.

The difference in compositional functional groups between RGO/PVDF and GO/PVDF membrane can be compared and confirmed by their FTIR spectra in Figure 4. The biggest difference was the intensity decrease of hydroxyl(—OH) peak at 3586 cm^{-1} in RGO/PVDF. The peaks around 1645 cm^{-1} attributed to the graphite backbone C=C and/or C=O, and the peak belonging to the C—O—C antisymmetric stretching vibration at 1072 cm^{-1} were weakened after HI treatment. The possible reaction mechanisms of hydroiodic acid with graphene oxide were the ring-opening reaction of epoxy groups and the substitution reaction of hydroxyl groups by halogen atoms.[30] In view of the above results, some C=C or C=O bonds may have been destroyed during thermal treatment with HI solution.

Raman spectroscopy is a good tool to investigate the strcutural changes in graphene sheets. Figure 5 showed the composite membranes all had two prominent peaks at ~1340 and ~1590 cm^{-1}, which belonged to the D and G bands, respectively. The disorder degree was usually evaluated by the area

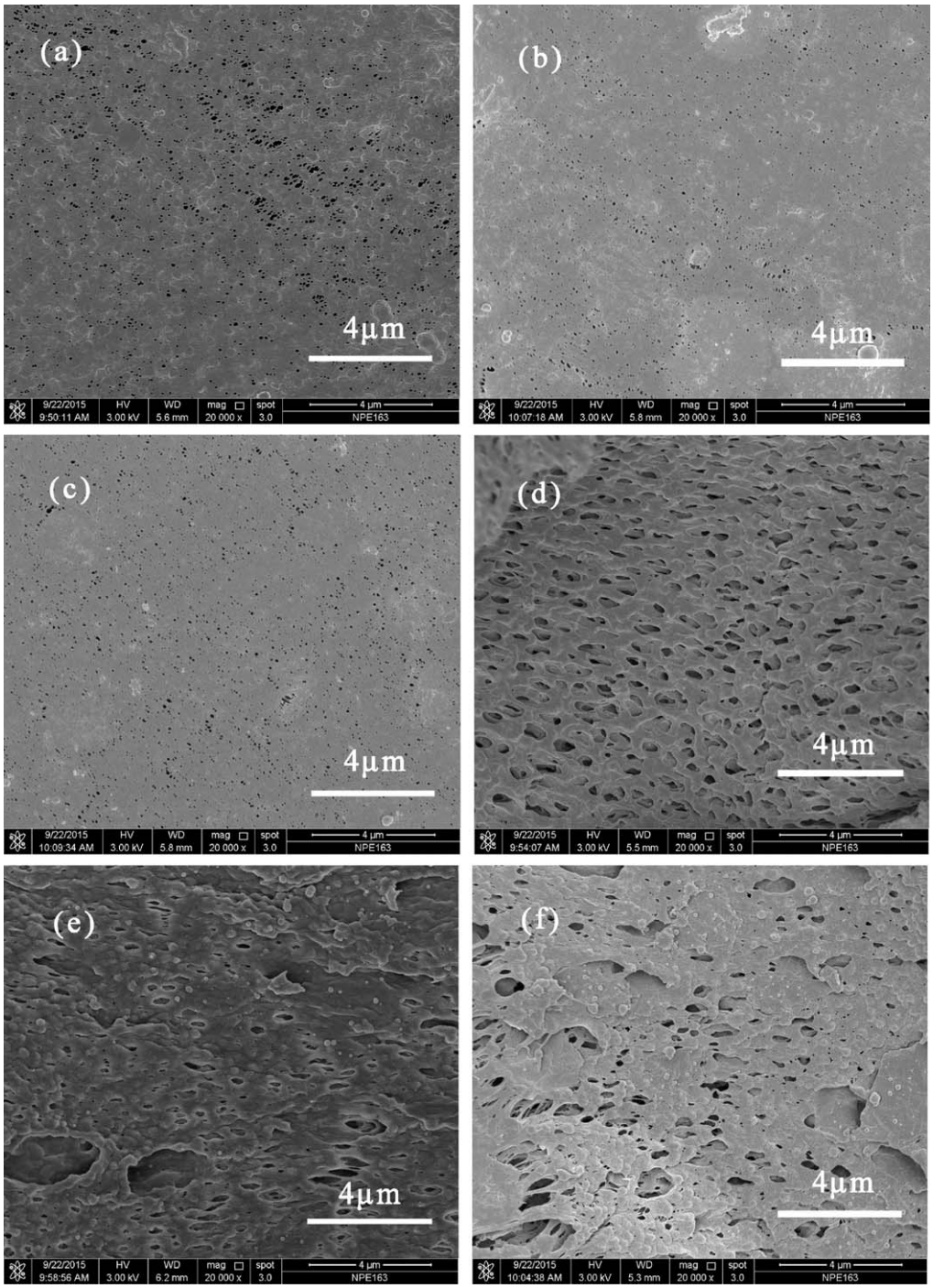

Figure 2. SEM images of the prepared membranes:surface and cross-section morphologies of (a,d) PVDF, (b,e) GO/PVDF, and (c,f) RGO/PVDF membranes.

ratio of D band to G band (I_D/I_G).[36,37] There is a slight decrease of I_D/I_G (from 0.903 to 0.865) after HI treatment, the result indicated a more ordered structure of RGO, and clearly supported the transformation from GO to RGO.

The thermogravimetric analysis(TGA) characterization had been conducted. From Figure 6, it is shown that the addition of GO and RGO improved the thermal stability of the membranes, when temperature was lower than 400 °C. Pure PVDF membrane begins to decompose at about 325 °C, but the GO/PVDF and RGO/PVDF membranes appear to degrade at 425 °C. The TGA-measured weight loss of GO is higher than that of RGO, about 45% for GO and 15% for RGO at 200 °C, nearly 53% for GO and 21% for RGO at 300 °C,[38] so the RGO/PVDF membrane had less weight loss, the results indicate the reduction of GO to RGO had occurred. Above 480 °C, the change profiles in weight loss were almost the same.

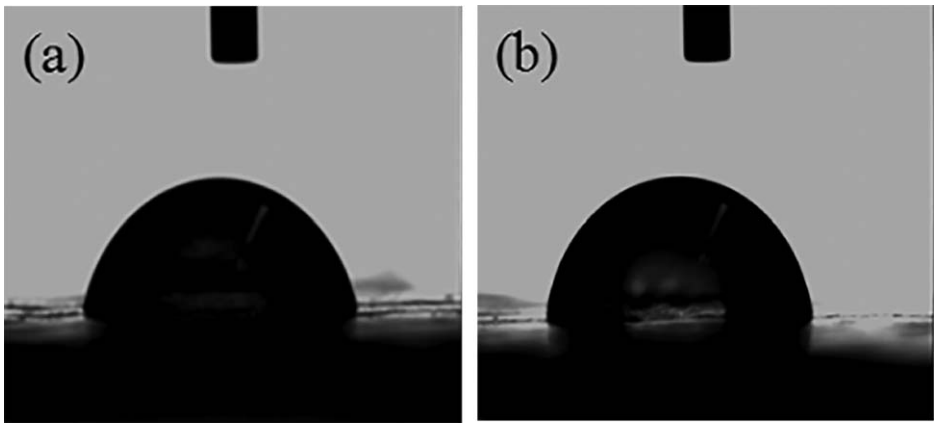

Figure 3. Water contact angles of the tested membranes: (a) GO/PVDF with contact angle of 76.5 ± 1.7°; (b) RGO/PVDF with contact angle of 83.1 ± 2.1°.

RGO had good conductivity, the RGO/PVDF membrane after HI treatment has about two orders increase in conductivity, from (0.72 ± 0.13) × 10^3 KΩ cm^{-1} to 7.3 ± 2.1 KΩ cm^{-1}. This thermal reduction transformed the low conductivity GO/PVDF surface layer on the carbon fiber cloth into a more conductive one. It is better for the separation of charged substances.

Filtration Performance and Fouling Resistance of the RGO/PVDF Membrane

Pure Water Flux. As mentioned in Refs 33,34, addition of GO increased the viscosity of casting solution, which lowered fluxes of GO/PVDF compared with pristine PVDF membrane. However, the pure PVDF surface layer without any conductivity had faster fouling rate (Figure 7). Although the hydrophilic GO was reduced after HI treatment, RGO/PVDF membrane had higher water flux, as shown in Figure 7. The pure water flux of pristine PVDF membrane after HI treatment increased about 18%, while RGO/PVDF membrane had 71.6% higher flux than GO/PVDF membrane. High flux membrane had more advantages in filtration.

Effects of External Electric Field on the Membrane Filtration Performance. ***Filtration of PAM solution.*** To ensure the unity of the variables, two membrane modules were put into filtration device at the same time, one was charged by direct-current (DC) power as cathode, another without DC power. Siphon effect was used to draw out water at a constant transmembrane pressure (TMP) at 9.8 kPa.

To compare the PAM filtration performance of GO/PVDF membrane with that of RGO/PVDF membrane, two sets of experiments were conducted. The results showed RGO/PVDF membrane had a higher filtration flux under 0.6 V/cm electric field. The rejection of PAM was similar and flux recovery rate (FRR) was higher for RGO/PVDF than GO/PVDF membrane (Figure 8). To GO/PVDF membrane, applying electric field did not make any difference in flux or rejection of PAM, it was probably due to the low conductivity of surface layer, which could not increase electrostatic repulsion between PAM and the membrane surface. When filtrating PAM without an external electric field, a slower flux decrease was observed for more

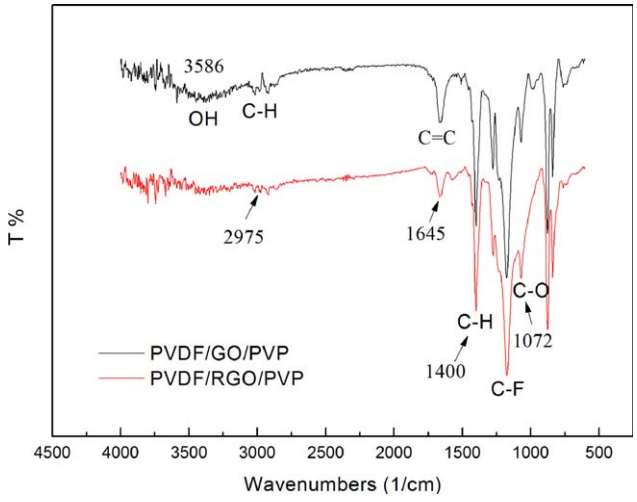

Figure 4. FTIR spectra of PVDF/GO and PVDF/RGO membranes. [Color figure can be viewed in the online issue, which is available at wileyonlinelibrary.com.]

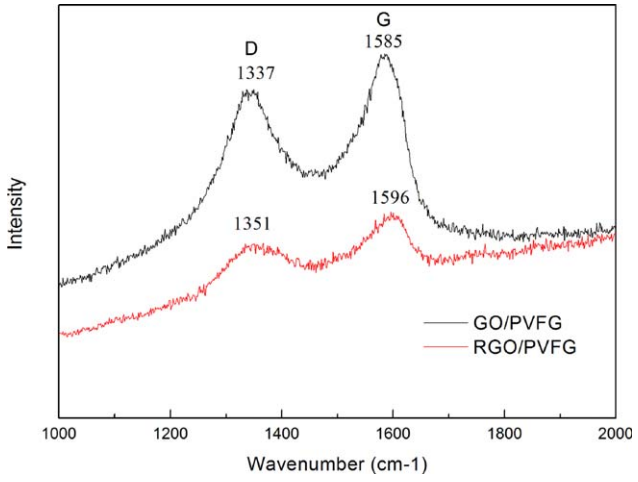

Figure 5. Raman spectra of PVDF/GO and PVDF/RGO membranes. [Color figure can be viewed in the online issue, which is available at wileyonlinelibrary.com.]

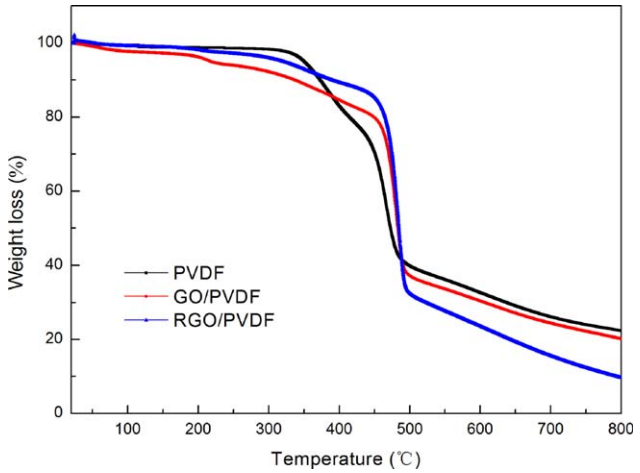

Figure 6. Thermograms of the prepared membranes in a nitrogen atmosphere with a heating rate of 10 °C/min. [Color figure can be viewed in the online issue, which is available at wileyonlinelibrary.com.]

hydrophilic GO/PVDF membrane than RGO/PVDF. The FRR value indicated fewer foulant remained on the RGO/PVDF membrane after cleaning (c).

With improved membrane conductivity, three cycles filtration experiments were carried out for the RGO/PVDF membrane. As shown in Figure 9(a), the normalized flux (J/J_0) under an applied electric field (0.6 V/cm) declined slowly than the control test (0 V/cm). The RGO/PVDF conductive membrane had a high rejection of PAM, but the rejection decreased when applying an electric field, as shown in Figure 9(b). This is probably caused by reduction in fouling which resulted in cleaner pore and low resistance in filtration. First, the presence of electric field had a positive influence on mitigating membrane fouling by PAM. PAM macromolecules (Zeta potential at −20 to −40 mV) were negatively charged, due to electrostatic repulsion between PAM and the charged membrane, fewer pollutants would deposit or block membrane pores by attaching on membrane surface. The low rate of clogging led to lower trapping/retention efficiency. Second, during the three filtration cycles, the rejection rate increased, this was certainly related to pore blocking and the formation of cake layer/or gel layer on membrane surface due to the viscous nature of the PAM macromolecule. Although tested membranes were briefly cleaned after filtration, which only remove the easily removable top layer

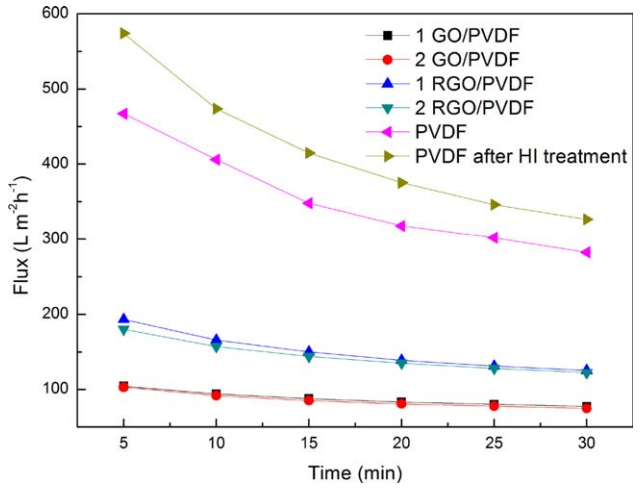

Figure 7. Pure water flux of different membranes. [Color figure can be viewed in the online issue, which is available at wileyonlinelibrary.com.]

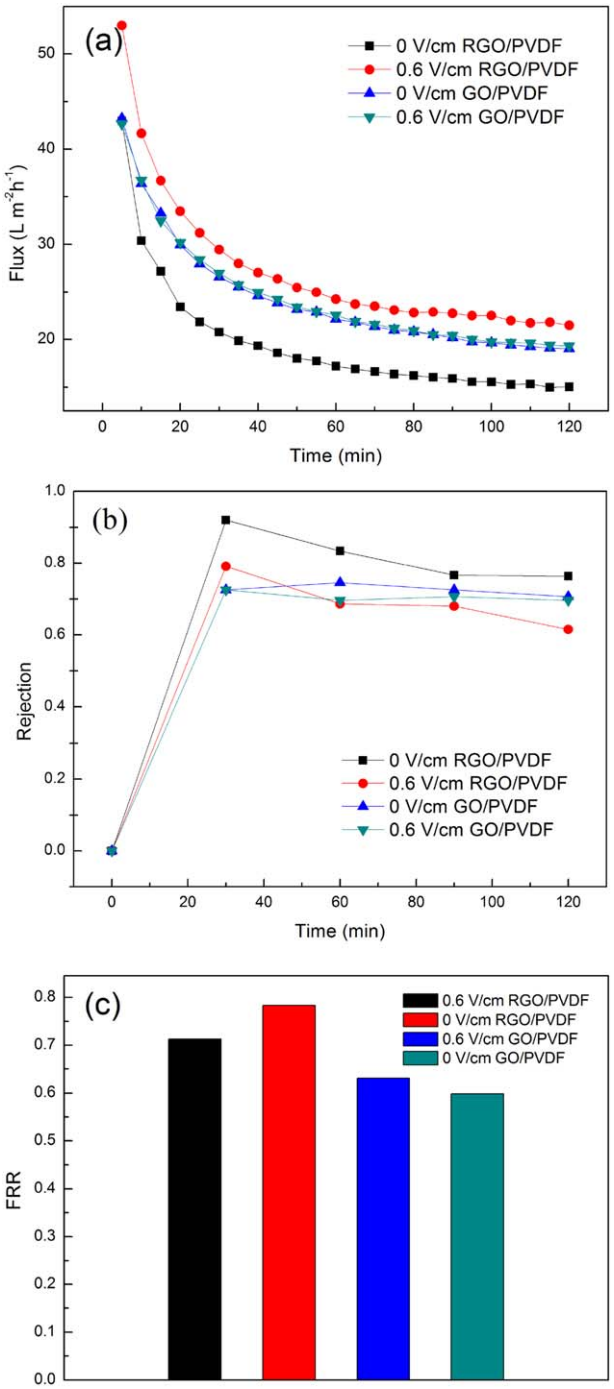

Figure 8. Filtration performance of RGO/PVDF and GO/PVDF membranes with PAM as target: (a) F-t; (b) R-t; (c) the flux recovery rate (FRR) after filtration. [Color figure can be viewed in the online issue, which is available at wileyonlinelibrary.com.]

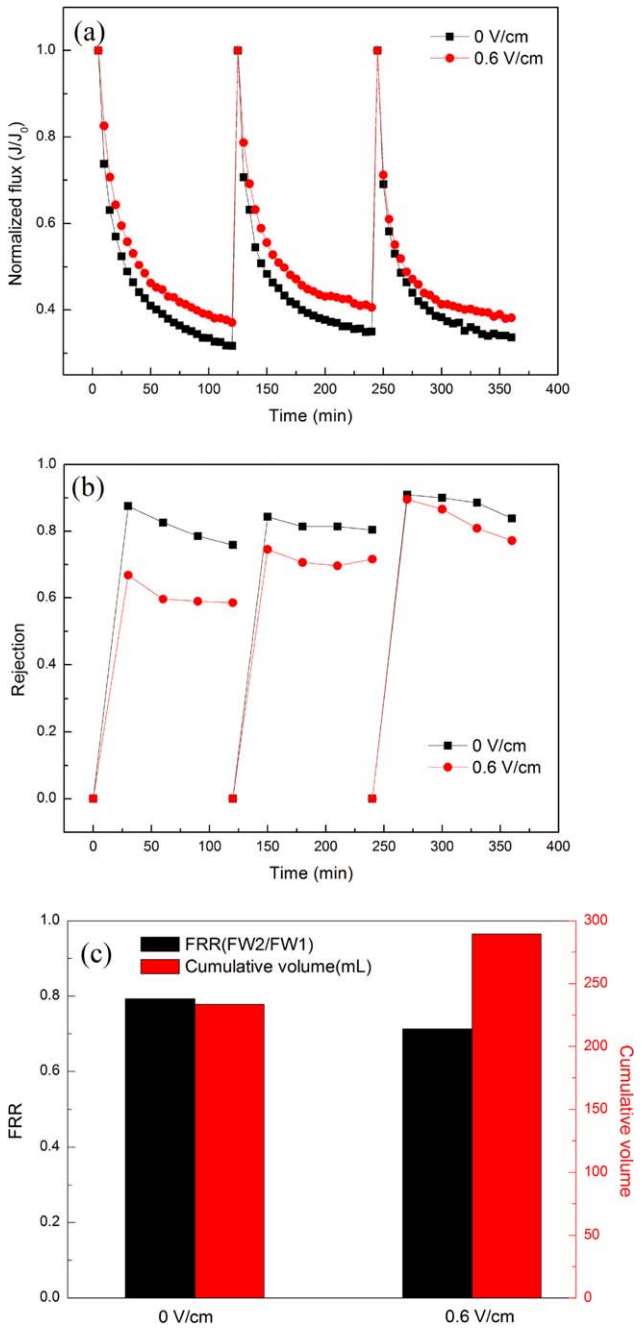

Figure 9. Filtration performance of RGO/PVDF membranes with PAM as target: (a) F-t; (b) R-t; (c) the average value of flux recovery rate (FRR) and corresponding cumulative volume of RGO/PVDF membrane in one filtration cycle. [Color figure can be viewed in the online issue, which is available at wileyonlinelibrary.com.]

(Rc), some residues remained (Rir and Rr). So, in cycle 3, it had the best rejection.

With respect to the difference in rejection of PAM by the applied electric field, the rejection was high in the first cycle, then the pore became narrower and smaller. PAM entered the membrane pores easier after initial membrane surface adsorption. Due to the accumulation of PAM, it was more easily trapped by the narrowed pores, or just adhered on the deposit PAM, thus the rejection and retention became higher.

As shown in Figure 9(c), applying an electric field increased the cumulative filtrate volume, but FRR values were similar. The increased filtrate volume was due to increased flux and decreased fouling by the electrostatic rejection force between membrane surface and PAM. While similar flux recovery was related to the nature of RGO/PVDF membrane, less PAM remained on membrane after cleaning [Figure 9(c)]. In summary, the conductive composite RGO/PVDF membrane had good antifouling performance.

The Mechanism of Membrane Fouling by PAM. The classical cake filtration model [t/V–V, (1)] and standard pore clogging filtration model [t/V–t, (2)] was compared for filtration with PAM.[21,39] The classical cake filtration model is applicable for describing fouling caused by deposition of particles on membrane surface, and formation of cake layer. While, the standard filtration model explains membrane fouling caused by pore clogging. Model formulas are as follows:

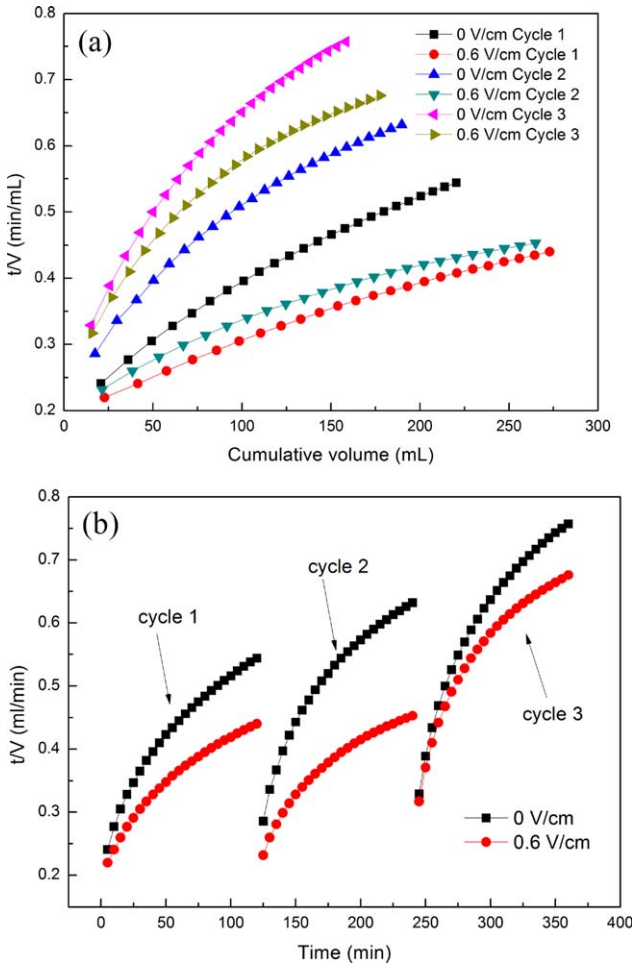

Figure 10. The (a) t/V-V and (b) t/V-t graphs of PAM in three-cycle filtration. [Color figure can be viewed in the online issue, which is available at wileyonlinelibrary.com.]

Table II. The Slopes and Linear Correlation Coefficients (R^2) of the Curves of RGO/PDVF Corresponding to Figure 7(b), the Pore Blocking Model

	$E = 0$ V/cm		$E = 0.6$ V/cm	
Filtration cycle	Slope (k, E-3)	R^2	Slope (k, E-3)	R^2
1st	2.40	0.949	1.79	0.956
2nd	2.66	0.924	1.74	0.933
3rd	3.28	0.920	2.70	0.901

$$\frac{t}{V} = \frac{1}{Q_0} + \frac{K}{2}V \quad (1)$$

$$\frac{t}{V} = \frac{1}{Q_0} + \frac{k}{2}t \quad (2)$$

Where t is the filtration time (min), V is the cumulative permeate volume over time (mL), Q_0 is the initial flux rate (L/min), K is the cake filtration constant, and k is the filtration constant (L^{-1}). For the models, when the values of K and k are smaller, the membrane fouling is lower.

According to Figure 10 and the fitting line slopes in Tables I and II, both models fit the PAM fouling on RGO/PVDF membrane, the cake layer model being a better fit. The membrane fouling process with PAM better fitted the classical model (t/V–V (1)). Because the PAM fouling of MF RGO/PVDF membrane proceeded by surface adsorption, deposition of gel layer and accumulation of cake layer, narrowed the pores eventually. The conductive composite membrane under electric field had the smallest slope (Tables I and II). Applying electric field on the conductive membrane could successfully slow down membrane fouling.

In fact, for removing polyacrylamide, some researches had been carried out, such as Fenton oxidation[40–42] and electrocatalytic oxidation.[43,44] These methods can degrade PAM in a short time, but the cost is high. Some researchers have separated bacteria for PAM degradation,[45–47] this is low cost and sustainable; however, the time consumed is long, and it need large volume facility. Compared with above-described methods, using membrane separation to recover PAM is not only time-saving and cost-saving but also efficient (80–90%). Meanwhile, the filtration membranes could be reused in cycles, for the membrane conductivity still was kept at 8.4 ± 1.2 kΩ cm^{-1}, and membrane showed good strength and toughness.

Table I. The Slopes and Linear Correlation Coefficients (R^2) of the Curves for RGO/PVDF Corresponding to Figure 8(a), the Cake Layer Model

	$E = 0$ V/cm		$E = 0.6$ V/cm	
Filtration cycle	Slope (K, E-3)	R^2	Slope (K, E-3)	R^2
1st	1.46	0.984	0.865	0.986
2nd	1.87	0.962	0.861	0.966
3rd	2.79	0.958	2.02	0.937

The carbon fiber cloth substrate had good conductivity, after coating of PVDF, the composite membranes have strong mechanical properties and chemical stability. Due to the conductivity of RGO/PVDF membrane, coating catalyst on the membrane could electrochemically catalyze degradation of pollutants by electrocatalytic oxidation, and couple MBR with MFC can realize energy saving.[22,23] Therefore, its further wide application is envisioned in water and waste water treatment with good prospects.

CONCLUSIONS

A conductive composite microfiltration RGO/PVDF membrane was prepared using carbon fiber cloth as substrate, by casting, nonsolvent phase inversion and thermal treatment in HI solution. SEM images showed that the added GO reduced the pore size of the composite membranes. FTIR and Raman spectroscopy indicated that the GO blended in PVDF layer was partially reduced to more conductive RGO after treatment in HI solution. Although this process made the prepared membrane less hydrophilic, but both the RGO and the membrane become more conductive and stable. TGA indicated the addition of GO and RGO improved the thermal stability of the membranes, when temperature was lower than 400 °C.

The HI treatment not only increased membrane conductivity but also enhanced pure water flux by 71.6% comparing with the GO/PVDF membrane. A high rejection percentage of PAM was achieved in filtration. When functioned as cathodes, the RGO/PVDF membrane had better antifouling performance under 0.6 V/cm applied electric field. The membrane fouling by PAM, fitting the classical cake filtration model, was reduced by applied electric field. Compared with the chemical and biological method for removing PAM, membrane separation is not only time-saving and cost-saving but also efficient. The low-cost material and stable operation suggested a promising future for this new membrane in practical applications.

ACKNOWLEDGMENTS

Authors acknowledge the financial support from China National Natural Science Foundation (Project No. 21177018).

AUTHOR CONTRIBUTIONS

Yuehua Zhang contributed to the manuscript in writing the draft paper, drawing figures, and obtained the data by testing. Lifen Liu supervised the research plan and revised the paper, and prof. Fenglin Yang supported in discussion and suggestions.

REFERENCES

1. Girard, B.; Fukumoto, L. R. *Crit. Rev. Food Sci. Nutr.* **2000**, *40*, 91.
2. Saxena, A.; Tripathi, B. P.; Kumar, M. *Adv. Colloid Interf. Sci.* **2009**, *145*, 1.
3. Stamatialis, D. F.; Papenburg, B. J.; Gironés, M. *J. Membr. Sci.* **2008**, *308*, 1.
4. Basu, S.; Khan, A. L.; Cano-Odena, A.; Liub, C. Q.; Vankelecom, I. F. J. *Chem. Soc. Rev.* **2010**, *39*, 750.

5. Kang, G. D.; Cao, Y. M. *J. Membr. Sci.* **2014**, *463*, 145.
6. Rao, A. P.; Desai, N. V.; Rangarajan, R. *J. Sci. Ind. Res.* **1997**, *56*, 518.
7. Yang, Y.; Li, J.; Wang, H. *Angew. Chem. Int. Ed.* **2011**, *50*, 2148.
8. Ang, W. S.; Tiraferri, A.; Chen, K. L.; Elimelech, M. *J. Membr. Sci. 376*, 196.
9. Zumbusch, P. V.; Kulcke, W.; Brunner, G. *J. Membr. Sci.* **1998**, *142*, 75.
10. Brunner, G.; Okoro, E. *Ber. Bunsenges Phys. Chem.* **1989**, *93*, 1026.
11. Hashaikeh, R.; Lalia, B. S.; Kochkodan, V. *J. Membr. Sci.* **2014**, *471*, 149.
12. Wang, S.; Liang, S.; Liang, P. *J. Membr. Sci.* **2015**, 491.
13. Zhang, Q. Y.; Vecitis, C. D. *J. Membr. Sci.* **2014**, *143*, 459.
14. Dudchenko, A. V.; Rolf, J.; Russell, K. *J. Membr. Sci.* **2014**, *468*, 1.
15. Yokwana, K.; Gumbi, N.; Adams, F.; Mhlanga, S. *J. Appl. Polym. Sci.* **2015**, *41835*, 1.
16. An, J.; Cui, J. F.; Zhu, Z. Q. *J. Appl. Polym. Sci.* **2014**, *40759*, 1.
17. Huang, J.; Wang, Z. W.; Zhang, J. Y. *Sci. Rep.* **2015**, 5.
18. Liu, L. F.; Liu, J. D.; Gao, B. *J. Membr. Sci.* **2013**, *429*, 252.
19. Liu, L. F.; Liu, J. D.; Gao, B. *J. Membr. Sci.* **2012**, *394395*, 202.
20. Liu, L. F.; Zhao, F.; Liu, J. D. *J. Membr. Sci.* **2013**, *437*, 99.
21. Li, N.; Liu, L. F.; Yang, F. L. *Desalination* **2014**, *338*, 10.
22. Li, Y. J.; Liu, L. F.; Liu, J. D.; Yang, F. L. *Desalination* **2014**.
23. Li, Y. H.; Liu, L. F.; Yang, F. L. *J. Membr. Sci.* **2015**, *484*, 27.
24. Lee, Y. R.; Kim, S. C.; Lee, H. *Macromol. Res.* **2011**, *19*, 66.
25. Hassan, M.; Reddy, K. R.; Haque, E. *Compos. Sci. Technol.* **2014**, *98*, 1.
26. Choi, S. H.; Kim, D. H.; Raghu, A. V. *J. Macromol. Sci. B Phys.* **2012**, *51*, 197.
27. Zhao, X.; Liu, L.; Wang, Y. *Sep. Purif. Technol.* **2008**, *62*, 199.
28. Hummers, W. S.; Offeman, R. E. *J. Am. Chem. Soc.* **1958**, *80*, 1339.
29. Pei, S. F.; Zhao, J. P.; Du, J. H. *Carbon* **2010**, *48*, 4466.
30. Mohan, V. B.; Brown, R.; Jayaraman, K. *Mater. Sci. Eng. B* **2015**, *193*, 49.
31. Zhao, J. P.; Pei, S. F.; Cheng, H. M. J. *ACS Nano* **2010**, *4*, 5245.
32. Reddy, A. V. R.; Patel, H. R. *Desalination* **2008**, *221*, 318.
33. Zhao, C. Q.; Xu, X. C.; Chen, J. *J. Environ. Chem. Eng.* **2013**, *1*, 349.
34. Chang, X. J.; Wang, Z. X.; Quan, S. *Appl. Surf. Sci.* **2014**, *316*, 537.
35. Sun, H.; Zhu, Z.; Liang, W.; Yang, B.; Qin, X.; Zhao, X.; Pei, C.; La, P.; Li, A. *RSC Adv.* **2014**, *4*, 30587.
36. Pei, S.; Ai, F.; Qu, S. *RSC Adv.* **2015**, *5*, 99841.
37. Bai, Z.; Li, H.; Li, M. *Int. J. Hydrogen Energy* **2015**, *40*, 16306.
38. Olowojoba, G. B.; Eslava, S.; Gutierrez, E. S. Nanotech France **2016**, 1.
39. Al-Malack, M. H.; Bukhari, A. A.; Abuzaid, N. S. *J. Membr. Sci.* **2004**, *243*, 143.
40. Cao, C.; Zhao, Y.; Zhou, Y. *Int. J. Green Energy* **2016**, *13*, 80.
41. Giroto, J. A.; Teixeira, A.; Nascimento, C. A. O. *Chem. Eng. Process. Process Intensificat.* **2008**, *47*, 2361.
42. Cao, C.; Zhao, Y.; Zhou, Y. *Int. J. Green Energy* **2016**, 1.
43. Giroto, J. A.; Teixeira, A.; Nascimento, C. A. O. *Chem. Eng. Process. Process Intensificat.* **2008**, *47*, 2361.
44. Yongrui, P.; Zheng, Z.; Bao, M.; Li, Y.; Zhou, Y.; Sang, G. *Chem. Eng. J.* **2015**, *273*, 1.
45. Yang, L. J.; Li, Y. Y.; Tian, M. *Adv. Mater. Res.* **2012**, *581*, 64.
46. Chen, W.; Yang, C.; Mei, P. *Wuhan Univ. J. Nat. Sci.* **2007**, *12*, 353.
47. Ren, G. M.; Pan, Y.; Yang, X. M. *Appl. Mech. Mater.* **2014**, *675*, 539.